Stochastic and deterministic switches in a bistable polariton micropillar under short optical pulses

A. V. Uvarov,[1,2,3] S. S. Gavrilov,[3,4] V. D. Kulakovskii,[3,4] and N. A. Gippius[2,3]
[1]*Moscow Institute of Physics and Technology, Moscow 117303, Russia*
[2]*Skolkovo Institute of Science and Technology, Skolkovo 143025, Russia*
[3]*Institute of Solid State Physics, RAS, Chernogolovka 142432, Russia*
[4]*National Research University Higher School of Economics, 101000 Moscow, Russia*

(Received 13 September 2018; published 18 March 2019)

Optical bistability of exciton polaritons in semiconductor microcavities is a promising platform for digital optical devices. Steady states of coherently driven polaritons can be toggled back and forth in tens of picoseconds under short external pulses of appropriate amplitude and phase. We have analyzed the switching behavior depending on the pulse amplitude, phase, and duration. The switches are found to change dramatically when the inverse pulse duration becomes comparable to the frequency detuning between the driving field and polariton resonance. If the detuning is large compared to the polariton linewidth, the system becomes extremely sensitive to initial conditions and thus responds unpredictably.

DOI: 10.1103/PhysRevA.99.033837

I. INTRODUCTION

This study is devoted to the transient processes that accompany nonequilibrium transitions in bistable cavity-polariton systems. Cavity polaritons are short-lived composite bosons originating due to the strong coupling of two-dimensional excitons and photons confined in a planar semiconductor microcavity [1]. At low temperatures they form a Bose-Einstein condensate in equilibrium with excitonic reservoir [2,3]. On the other hand, macroscopically coherent polariton states can be immediately created and maintained by resonant and coherent optical driving [4,5]. These two types of polariton condensates are similar in the sense of quantum statistics, yet they have different origins and thus behave differently with respect to changing environment, temperature, or pumping parameters.

Repulsive interaction of polaritons with parallel spins brings about a variety of collective effects: self-organized parametric oscillations [6–9], spin rings [10–13], and bright solitons propagating without dissipation in spite of a very small lifetime of individual particles [14–17]. All these phenomena take place under resonant driving and imply optical multistability of macroscopic polariton states. In contrast to conventional lasers in which the multistable behavior is caused by nonlinear gain or decay rate of light [18], polariton multistability stems from a blueshift of eigenfrequencies with growing amplitude (in analogy to Bose-Einstein condensates of cold atoms [19]). If the pump frequency is initially set above resonance, then increasing power beyond a certain threshold enables switching the system into the high-intensity state in which the frequency detuning is effectively compensated by the polariton blueshift, resulting in a pronounced hysteresis behavior [20–28].

Similar to a simple damped pendulum, the switching time of the driven polariton mode is comparable to its lifetime (or inverse decay rate) and is of the order of 10 ps in GaAs-based microcavities. This duration is much shorter than in lasers or cavities without the strong light-matter interaction (see, e.g., [29–33]). As a consequence, polariton systems have attracted much attention in view of fast optical switches and logic gates [34]; for instance, an all-optical implementation of a polariton transistor has been demonstrated [35]. To create a conventional switch, one usually needs a two-beam excitation scheme in which one beam is a plane wave maintaining multistability and the other is a short pulse that acts as a trigger of transitions between steady states. One such scheme was implemented based on the spin anisotropy of the polariton-polariton interaction so that different transitions occur in response to pulses with different optical polarizations [36,37]. The other proposed way to implement switches relies upon ultrafast acoustic rather than optical pulses which disturb the resonance energy [38,39]. In a spatially distributed system, short pulses result in bright solitons or a neuronlike propagation [40,41] of the high-intensity state.

In this work we investigate the possibility to toggle a bistable polariton system back and forth by short optical pulses which are co-polarized with the background continuous-wave (cw) laser beam; in other words, we do not employ the spin degrees of freedom. Similar to Refs. [36,37], we focus our attention on a micron-sized pillar which is known to behave like an isolated nonlinear oscillator due to the size quantization effect. In the general case, the relative phase of the incident pulse is the key parameter which is hard to control. We have found, however, that in a certain parameter range the transitions can also be phase insensitive. In particular, within an interval of comparatively great pulse amplitudes the upward transitions turn out to be forbidden irrespective of the pulse phase. Surprisingly enough, such transitions are prevented even when the continuous wave and the pulse interfere positively. This finding allows one to perform a backward transition under a sequence of short pulses with random phases.

In a different interval of pulse amplitudes, the basins of attraction of two steady states are, by contrast, interlaced very

tightly and the outcome of each particular pulse becomes unpredictable at small decay rates. Thus, we show that a micropillar disturbed by short optical pulses can exhibit a nondeterministic regime of operation, in addition to the usual deterministic switching regime.

The paper is organized as follows. In Sec. II we introduce the model based on the Gross-Pitaevskii equation and its single-mode approximation suitable for describing polariton states in a micropillar. Section III describes typical phase trajectories under short optical pulses. In Sec. IV we consider two qualitatively different regimes of evolution which are well separated in the phase space. In Sec. V we summarize.

II. MODEL

A. Gross-Pitaevskii equation

Polaritons in semiconductor microcavities are mixed states of cavity photons and two-dimensional excitons confined in quantum wells. The polariton spectrum is split into two dispersion curves, lower and upper polariton branches

$$\omega_{\mathrm{LP,UP}} = \tfrac{1}{2}[\omega_{\mathrm{cav}}(\mathbf{k}) + \omega_{\mathrm{exc}}(\mathbf{k})] \mp \tfrac{1}{2}\sqrt{[\omega_{\mathrm{cav}}(\mathbf{k}) - \omega_{\mathrm{exc}}(\mathbf{k})]^2 + \Omega_R^2}, \quad (1)$$

where Ω_R is the Rabi splitting (the rate of the exciton-photon interactions).

In order to localize polaritons at a certain place, the cavity mirrors can be etched out except for the micropillar of a particular size; in so doing polaritons retain a high-Q factor [22,36]. When the pillar has a radius of several microns, the continuous polariton spectrum turns into a set of discrete energy levels due to size quantization. In planar cavities, the dynamics of the macroscopic wave function $\psi(\mathbf{r}, t)$ obeys the Gross-Pitaevskii equation (GPE) with the free term representing external driving [8,42] and a sharp change in energy $U(\mathbf{r})$ simulating the pillar boundary

$$i\frac{\partial \psi}{\partial t} = [\omega_{\mathrm{LP}}(-i\nabla) - i\gamma + U(\mathbf{r}) + V_a|\psi|^2]\psi + f_a(\mathbf{r}, t)e^{-i\omega_p t}, \quad (2)$$

where V_a is the polariton repulsion energy per unit area, ω_p and f_a are the pump frequency and amplitude per unit area, respectively, and γ is the polariton decay rate (damping coefficient). The units of ψ are chosen in such a way that $V_a = 1$. We assume that the pump is circularly polarized and neglect the spin degree of freedom.

This model is rather simplified, as we dropped the upper polariton branch and neglected the dependence of V_a on the wave vectors of the interacting waves. However, this simplification does not invalidate our conclusions because the pump frequency is supposed to be close to the lowermost eigenstate and consequently (i) the upper polariton branch is too far to have any significant influence and (ii) the lowest eigenmode of the pillar contains most of the wave-function density and lies in the k-space area where the discrepancy caused by the simplification of V_a is minimal. Hence, the error appears mostly in other modes, which should not affect the results qualitatively. Nonetheless, one should keep in mind that such simplification effectively enhances the polariton-polariton interaction and therefore it only gives the upper estimate of the impact of remote wave vectors.

The polariton system is known to exhibit bistable behavior if the pumping amplitude f is constant and the frequency detuning $D = \omega_p - \omega_{\mathrm{LP}}$ is larger than $\sqrt{3}\gamma$ [4,20]. The switching between such states is realized by adding a short pulse to the constant driving field

$$f_a = f_0 + f_1 \times 2^{-(t-t_0)^2/2\tau^2}. \quad (3)$$

Here f_1 is complex valued, so it contains information about the phase difference of cw pumping and the pulse: $f_1 = |f_1|\exp(-i\phi)$. The full width at half maximum (FWHM) of the pulse equals 2τ.

B. Single-mode approximation of a micropillar

The core assumption underlying the single-mode approximation is that all other modes are sufficiently far from the pump frequency so they do not affect the system behavior. Keeping that in mind and assuming that the pump is monochromatic (i.e., the time dependence of f is much slower than the oscillations at the pump frequency), we introduce an ansatz

$$\psi(\mathbf{r}, t) = \Psi(t)u_0(\mathbf{r})e^{-i\omega_p t} + \chi(\mathbf{r}, t), \quad (4)$$

where u_0 is the normalized wave function of the ground state in a circular potential well and χ is the deviation of the solution shape from that of the ground state. This deviation is small compared to $\|\Psi u_0\| = |\Psi|$ when the pumping is weak and the nonlinear term of the GPE is negligible. Substituting (4) into (2) and projecting it on u_0 yields a single-mode equation for Ψ,

$$i\frac{\partial \Psi}{\partial t} = (-D - i\gamma)\Psi + V|\Psi|^2\Psi + f, \quad (5)$$

where $D = \omega_p - \omega_{\mathrm{LP}}(k = 0)$, $V = V_a\int |u_0|^4 dS$, and $f = \int u_0^* f_a dS$.

Equation (5) resembles the famous Duffing equation for a nonlinear oscillator with an amplitude-dependent resonance frequency. Note, however, that the nonlinear term in Eq. (5) represents a pure blueshift of the resonance; it is a particular case of the real-valued cubic term in the Duffing model $(\Psi + \Psi^*)^3$, which is also responsible for new oscillation harmonics arising under plane-wave excitation and eventually for dynamical chaos. Models (5) and (2) exhibit no self-pulsing or chaos unless they are modified taking into account two spin components [43–45] or have the self-focusing type of nonlinearity ($V < 0$) [46–49]. A spatially extended model (2) with $V > 0$ is known to have nontrivial evolution scenarios such as dynamics with blowup [50,51]. If the model is single mode, the evolution is comparatively trivial and always ends up in one of two steady states. Our goal is to investigate transitions between these states under short optical pulses.

III. PHASE TRAJECTORIES

In the absence of short-term pulses, Eq. (5) is autonomous. Its typical phase portrait is depicted in Fig. 1. The high- and low-amplitude steady states (labeled, respectively, "ON" and "OFF") are stable foci, while the unstable state is a saddle point (S). The phase picture contains the trajectories resulting in one of two steady states and thus shows the two

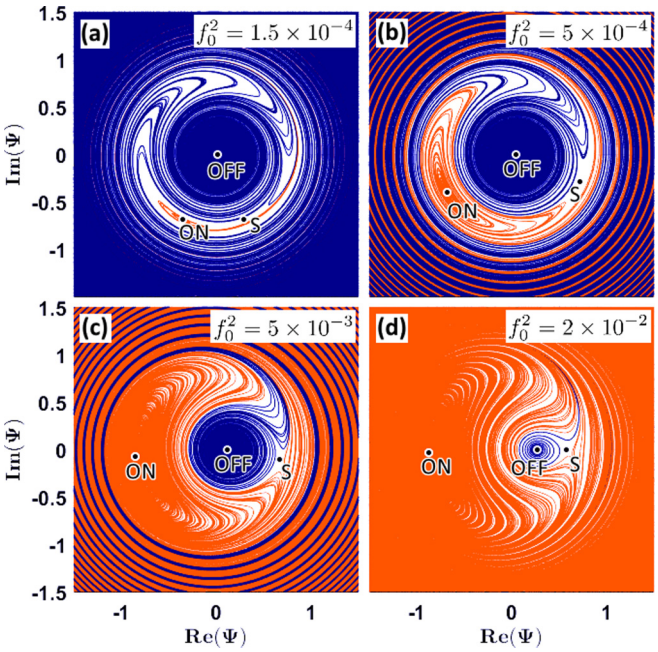

FIG. 1. Phase trajectories representing solutions of Eq. (5) with time-independent pump amplitude. Trajectories shown by red (bright) and blue (dark) curves are attracted to the ON and OFF states, respectively. Points highlight the stationary solutions: ON, OFF, and saddle point S. Here and in all other figures, unless stated otherwise, $\hbar D = 0.6$ meV, $\hbar\gamma = 0.014$ meV, and $V = 1$.

basins of attraction. With increasing pump amplitude f_0 [see Figs. 1(a)–1(d)] the area of the Ψ plane attracted to the ON state gradually grows. The ON state and the saddle point are drifting apart and in the limit of high amplitude they approach the real axis (Im $\Psi = 0$).

Let us consider the system excited with a short pulse and then relaxing to one of two steady states. Naturally, the resulting state depends on the pulse parameters. The evolution has three characteristic timescales: the decay time γ^{-1}, the pulse duration τ, and the inverse frequency of rotation in the phase space $T = |V|\bar{\Psi}|^2 - D|^{-1}$, where $\bar{\Psi}$ denotes a characteristic value of Ψ. The solution changes the most noticeably upon varying the ratio between the last pair of characteristic times, whereas γ^{-1} is assumed to largely exceed both of them. The smaller the pulse duration, the greater the pulse amplitude f_1 that is necessary to produce a pronounced effect on the system. However, the overall approach is no longer self-consistent when $\tau \ll T$. Indeed, if the pulse is short, its spectral width is high and thus the pulse will necessarily affect the eigenstates beyond the first one which are excluded from our consideration.

If, by contrast, $\tau \gg T$, then the driving field and phase plane change slowly, while Ψ evolves relatively rapidly. If, in addition, τ is comparable to γ^{-1}, the solution follows the equilibrium state adiabatically. In this case, the final state depends on how the system leaves the bistability region during the pulse. If the pump power is beyond the bistability turning point, the OFF state merely vanishes and thus the system can be reliably delivered to the ON state. The only exception occurs when the phase difference between the background cw pump and the pulse approximately amounts to π. In the latter case the two pump sources cancel each other and the overall intensity drops down to quite a low value before it is restored to the normal cw intensity. As a result, the system is delivered to the OFF state. This regime is consistent with the switching mechanism discussed in Ref. [37].

Let us now turn to the intermediate regime lying in between the above limiting cases, namely, $\tau \sim T$. During the switching pulse, one can imagine an instant phase plane with instant steady states and their basins of attraction. The absolute value of the ON point moves rapidly at the leading and trailing fronts of the pulse and slows down near the pulse maximum. Due to the strong blueshift of the resonance at high powers, $|\Psi_{\rm ON}|$ grows as a cubic root of the pumping amplitude. As a result, during the pulse the solution exhibits a rotation around the slowly drifting ON state in accord with the instantaneous magnitude of the total external field. After the switching pulse has turned off, Ψ gradually returns to one of the stationary states following the flow lines of the stationary phase plane.

This intermediate switching regime can be illustrated by the example of a pulse with amplitude f_1 turned on during a certain time τ (Fig. 2). The solution exhibits rotations around $\Psi_{\rm ON}$ with a negligible decay, and after the pulse has turned off the system goes along stable phase trajectories.

Given that the angle spanning around the ON point is the same up to 2π for two pairs (f_1, τ), the following trajectories are the same also and these pairs can be considered equivalent. The angular velocity of such rotation can be estimated by considering a perturbed solution near the ON state: $\Psi = \Psi_{\rm ON} + \delta\Psi$. If we substitute this expression into (5) and hold only the terms no smaller than $\delta\Psi$, we get

$$i\partial_t(\delta\Psi) = (-D - i\gamma)\delta\Psi + 2V\left(|\Psi_{\rm ON}|^2\delta\Psi + \Psi_{\rm ON}^2\delta\Psi^*\right). \quad (6)$$

Let $\delta\Psi = re^{i\theta}$; then, after separating the real and imaginary parts of the equation, we obtain

$$\dot{r} = V\,\mathrm{Im}\left(\Psi_{\rm ON}^2 e^{-2i\theta}\right)r - \gamma r, \quad (7)$$

$$\dot{\theta} = (D - 2V|\Psi_{\rm ON}|^2) + V\,\mathrm{Re}\left(\Psi_{\rm ON}^2 e^{-2i\theta}\right). \quad (8)$$

Equation (8) suggests that in the case of a very strong pumping the solution rotates clockwise (that is, $\dot{\theta} < 0$) and $-3V|\Psi_{\rm ON}|^2 < \dot{\theta} < -V|\Psi_{\rm ON}|^2$. Taking into account that, asymptotically, $|\Psi_{\rm ON}|^2 \sim f_1^{2/3}$, we have $|\dot{\theta}| \sim |f_1|^{2/3}$. If the solution has made a full circle around the $\Psi_{\rm ON}$ point, i.e., $2\pi n = \tau\dot{\theta} \sim \tau f_1^{2/3}$, the corresponding trajectories are equivalent. Thus, to estimate the amplitudes of the equivalent switching pulses in the phase space, one should solve this equation for f_1, which eventually yields $f_1^{(n)} \sim n^{3/2}$.

IV. STOCHASTIC AND DETERMINISTIC REGIMES

A. Response of the OFF state

We simulated the response of the single-mode system to the pulses in a wide parameter area. Each set of pulse amplitudes (Re f_1, Im f_1) and other parameters such as pulse duration τ or decay rate γ results in one of two states, ON or OFF, which can be indicated by different colors on the phase plane. An example of such mapping is seen in Fig. 3. In the series shown, τ increases from left to right. In the case of strong but very short pulses (with a duration much smaller than the inverse detuning) the value of Ψ immediately after the pulse

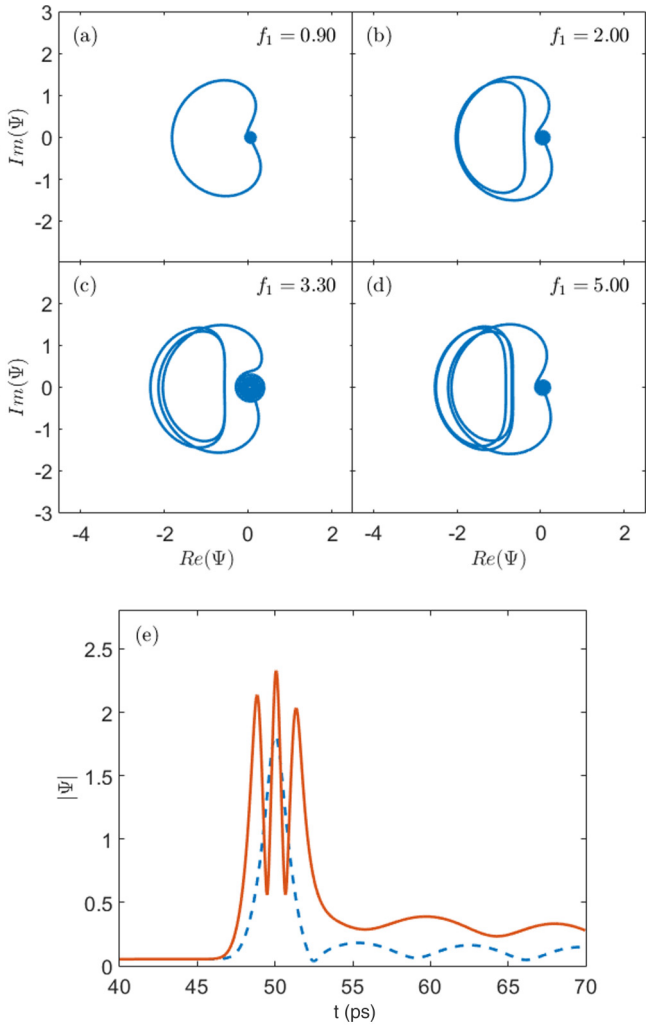

FIG. 2. (a)–(d) Four different trajectories that leave the system in the OFF state. (e) Explicit time dependences for $f_1 = 0.9$ (blue dashed line) and $f_1 = 3.3$ (orange solid line). In spite of making several loops with high $|\Psi|$ during the switching pulse, all these trajectories converge to the OFF state. Note as well that the central point of such rotations changes slowly compared to the pulse amplitude f_1. The FWHM of the pulses (τ) is 2 ps.

is proportional to f_1. Indeed, all terms on the right-hand side of Eq. (5) except the last one can be neglected in the course of the pulse action and the solution is thus approximated by an integral over the δ function. Consequently, the switching pattern seen in the f_1 plane resembles the Ψ plane (Fig. 1) drawn in accordance with the basins of attraction.

Figure 3(c) represents the opposite limiting case. Here different basins almost do not intermix, because the system adiabatically follows the "equilibrium" state determined by the pulse amplitude at each time moment. When f_1 is aligned in phase with the cw pump, the OFF state becomes unavailable and the solution sticks with the ON state. If, by contrast, f_1 counteracts the cw pump, there is a region where the ON state is unavailable, so the system returns to the OFF state after a number of oscillations. The fact that the system is not perfectly adiabatic manifests itself in the serrate border between the two regions: The transient oscillations do

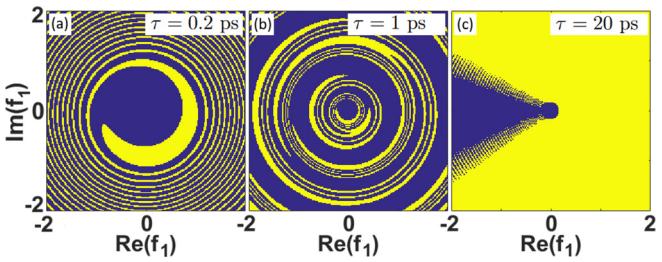

FIG. 3. Final states of evolution depending on the pulse amplitude for time (a) $\tau = 0.2$ ps, (b) $\tau = 1$ ps, and (c) $\tau = 20$ ps. The starting state is OFF. Yellow (bright) color means that the final state is ON, blue (dark) means that the final state is OFF. The background pump amplitude is $f_0^2 = 5 \times 10^{-4}$. All other parameters are fixed and equal to those in Fig. 1.

not smooth out completely during the pulse. The longer the lifetime, the more pronounced the serrate area of the phase space, which is illustrated in Fig. 4.

Figure 3(b) shows the final states for the intermediate pulse length. This picture exhibits a region where the characteristic spiral unwinds counterclockwise and then back in the opposite direction. This behavior is consistent with the explanation suggested above. With increasing $|f_1|$, the system initially reaches higher values of $|\Psi|$, but such states are highly unstable and after the pulse the amplitude decreases drastically. The appearance of the dark ring-shaped area corresponding to the OFF-state basin means that the result does not depend on the relative phase of the pulse. However, with increasing the background cw pump, the OFF-state basin shrinks and shifts away from the center. The ring gradually disappears, which is specifically illustrated in Fig. 5.

Thus, it turns out that both OFF and ON states can be reached irrespective of the pulse phase. The deterministic, i.e., phase-independent, upward transition is ensured by a stronger cw pump, which is quite expected. However, the deterministic choice of the lower state under strong short-term pulses in a wide interval of their amplitudes and irrespective of their phases might seem surprising.

The smaller the decay rate is, the greater the number of oscillations the system makes before arriving at the saddle point and falling into the vicinity of one of two focal points.

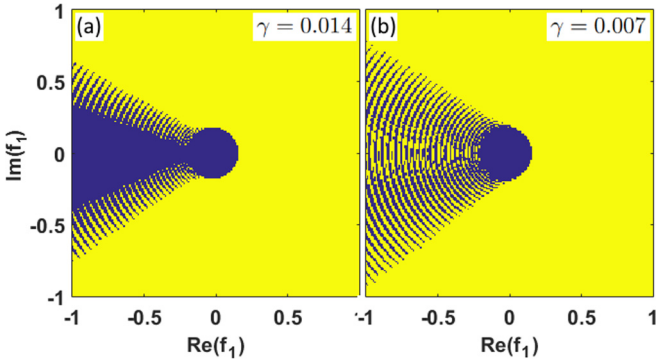

FIG. 4. Final states for $\tau = 20$ ps and two different values of decay rate γ: (a) $\gamma = 0.014$ and (b) $\gamma = 0.007$. The serrate boundary between the two regions becomes more pronounced with increasing γ.

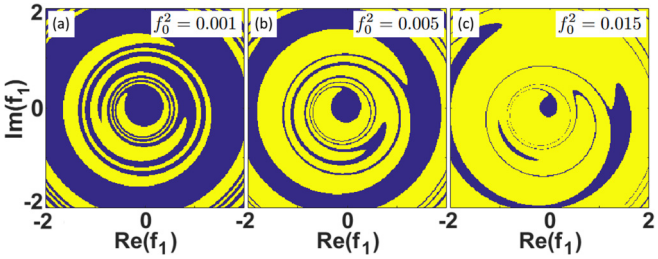

FIG. 5. Transformation of Fig. 3(b) with increasing amplitude f_0 of the background cw pump. Expectedly, the transition to the upper steady state becomes more probable with increasing pump amplitude.

In terms of the phase portraits seen in Figs. 3–5, this means an increased number of coils around the center. However, the outer part of the diagram stays more or less stable, including the ends of the spirals, the ring with the guaranteed OFF state, etc. In the limit of $\gamma \to 0$, there is a certain region where the density of the coils tends to infinity, which is specifically illustrated in Fig. 6. In this case the system shows a nondeterministic regime of response unless the pulse phase is known with infinite accuracy. In general, the system is biased to one of the two states depending on the background pump parameters, which opens up a way to manipulate the relative probability of the outcomes. Note that this regime coexists in the (Re f_1, Im f_1) phase space with the completely deterministic regime.

B. Response of the ON state

The considered approach can also be applied to the single-mode system whose evolution starts in the ON state. For clarity, the results are shown in Fig. 7(b) side by side with the already discussed case of the evolution starting in the OFF state. Now the pulse can drive the system down or leave in the ON state, depending on both amplitude and phase. Notice that the ON state is substantially off-center in the phase diagram (in accord with Fig. 1) and consequently

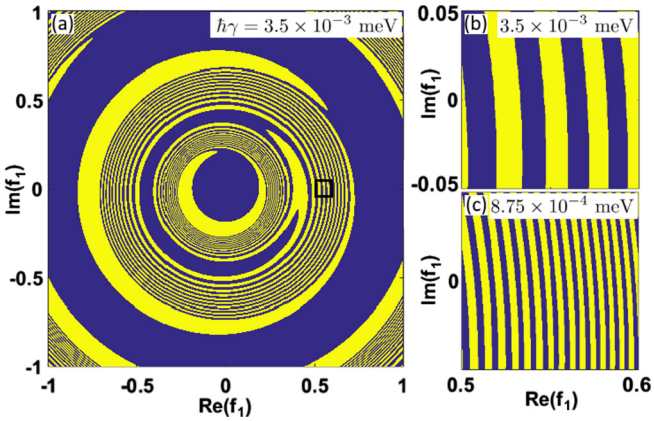

FIG. 6. (a) Final states in the case when $1/\gamma$ is much greater than other characteristic times of the system. Panels (b) and (c) magnify the area highlighted with the black square at different values of the decay rate. The parameters are $\tau = 1$ ps and $f_0^2 = 5 \times 10^{-4}$. With decreasing γ, the parameter areas resulting in the ON and OFF states are interlaced extremely tightly.

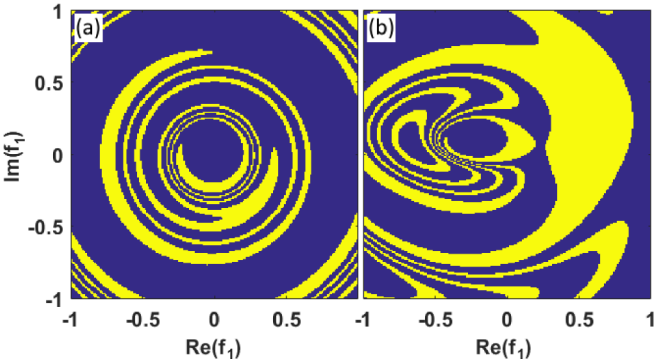

FIG. 7. Final states of the system in the cases when the starting state is (a) OFF and (b) ON. Notice the absence of the ring in latter case, which means that the outcome of a single pulse with unknown phase is not determined. The parameters are $f_0^2 = 5 \times 10^{-4}$ meV ps^{-2} and $\tau = 2$ ps.

there is no analog of the phase-independent ring-shaped area that would guarantee the backward transition after a single pulse with unknown phase. In order to perform the backward transition to the OFF state, one could apply a series of pulses with random phases, given that their amplitude lies within the ring seen in Fig. 7(a). Indeed, each of such pulses can drive the system down or leave unchanged, but definitely cannot drive it up from the OFF state. Thus, if one cannot control the pulse phases, it is still possible to perform a backward transition using a series of short-term pulses.

V. CONCLUSION

We have studied the driven polariton mode under the joint action of cw and pulsed pumping when the system is bistable and the short pulse acts as a trigger of transitions between steady states. The result is shown to be a nontrivial function of the pulse duration and amplitude. Depending on these parameters, several dynamical scenarios can be distinguished.

First, the pulse intensities resulting in the ON and OFF states can be tightly interlaced in the phase space. The intensity variation which is sufficient for altering the eventual steady state tends to zero with decreasing decay rate. Thus, for a pulsed laser with a finite accuracy of repetition, the response is essentially stochastic. The relative probabilities of the two outcomes depend on the cw pump intensity. The second type of solutions is, by contrast, deterministic. Within another area of the phase space, the system is guaranteed to stay in the OFF state after the pulse has gone, whereas the downward transition from the ON state can be ensured by a series of short-term pulses. The two types of solutions coexist for the same set of the microcavity parameters. With increasing pulse power, stochastic and deterministic regions are well separated in the phase space, which opens up the possibility of robust external control of the evolution scenario.

ACKNOWLEDGMENT

The study was partially supported by Volkswagen Foundation Grant No. 90418 and RFBR Grant No. 16-29-03333.

[1] C. Weisbuch, M. Nishioka, A. Ishikawa, and Y. Arakawa, Phys. Rev. Lett. **69**, 3314 (1992).

[2] J. Kasprzak, M. Richard, S. Kundermann, A. Baas, P. Jeambrun, J. M. J. Keeling, F. M. Marchetti, M. H. Szymanska, R. André, J. L. Staehli, V. Savona, P. B. Littlewood, B. Deveaud, and L. S. Dang, Nature (London) **443**, 409 (2006).

[3] H. Deng, H. Haug, and Y. Yamamoto, Rev. Mod. Phys. **82**, 1489 (2010).

[4] V. F. Elesin and Y. V. Kopaev, Zh. Eksp. Teor. Fiz. **63**, 1447 (1972) [Sov. Phys. JETP **36**, 767 (1973)].

[5] A. Baas, J.-P. Karr, M. Romanelli, A. Bramati, and E. Giacobino, Phys. Rev. Lett. **96**, 176401 (2006).

[6] R. M. Stevenson, V. N. Astratov, M. S. Skolnick, D. M. Whittaker, M. Emam-Ismail, A. I. Tartakovskii, P. G. Savvidis, J. J. Baumberg, and J. S. Roberts, Phys. Rev. Lett. **85**, 3680 (2000).

[7] R. Butté, M. S. Skolnick, D. M. Whittaker, D. Bajoni, and J. S. Roberts, Phys. Rev. B **68**, 115325 (2003).

[8] N. A. Gippius, S. G. Tikhodeev, V. D. Kulakovskii, D. N. Krizhanovskii, and A. I. Tartakovskii, Europhys. Lett. **67**, 997 (2004).

[9] A. A. Demenev, A. A. Shchekin, A. V. Larionov, S. S. Gavrilov, V. D. Kulakovskii, N. A. Gippius, and S. G. Tikhodeev, Phys. Rev. Lett. **101**, 136401 (2008).

[10] I. A. Shelykh, T. C. H. Liew, and A. V. Kavokin, Phys. Rev. Lett. **100**, 116401 (2008).

[11] D. Sarkar, S. S. Gavrilov, M. Sich, J. H. Quilter, R. A. Bradley, N. A. Gippius, K. Guda, V. D. Kulakovskii, M. S. Skolnick, and D. N. Krizhanovskii, Phys. Rev. Lett. **105**, 216402 (2010).

[12] C. Adrados, A. Amo, T. C. H. Liew, R. Hivet, R. Houdré, E. Giacobino, A. V. Kavokin, and A. Bramati, Phys. Rev. Lett. **105**, 216403 (2010).

[13] S. S. Gavrilov, A. S. Brichkin, A. A. Demenev, A. A. Dorodnyy, S. I. Novikov, V. D. Kulakovskii, S. G. Tikhodeev, and N. A. Gippius, Phys. Rev. B **85**, 075319 (2012).

[14] O. A. Egorov, D. V. Skryabin, A. V. Yulin, and F. Lederer, Phys. Rev. Lett. **102**, 153904 (2009).

[15] O. A. Egorov, D. V. Skryabin, and F. Lederer, Phys. Rev. B **84**, 165305 (2011).

[16] M. Sich, D. N. Krizhanovskii, M. S. Skolnick, A. V. Gorbach, R. Hartley, D. V. Skryabin, E. A. Cerda-Mendez, K. Biermann, R. Hey, and P. V. Santos, Nat. Photon. **6**, 50 (2012).

[17] M. Sich, F. Fras, J. K. Chana, M. S. Skolnick, D. N. Krizhanovskii, A. V. Gorbach, R. Hartley, D. V. Skryabin, S. S. Gavrilov, E. A. Cerda-Méndez, K. Biermann, R. Hey, and P. V. Santos, Phys. Rev. Lett. **112**, 046403 (2014).

[18] H. M. Gibbs, *Optical Bistability: Controlling Light with Light* (Academic Press, New York, 1985).

[19] L. Pitaevskii and S. Stringari, *Bose-Einstein Condensation and Superfluidity* (Oxford University Press, New York, 2016).

[20] A. Baas, J. P. Karr, H. Eleuch, and E. Giacobino, Phys. Rev. A **69**, 023809 (2004).

[21] N. A. Gippius, I. A. Shelykh, D. D. Solnyshkov, S. S. Gavrilov, Y. G. Rubo, A. V. Kavokin, S. G. Tikhodeev, and G. Malpuech, Phys. Rev. Lett. **98**, 236401 (2007).

[22] T. K. Paraïso, M. Wouters, Y. Léger, F. Morier-Genoud, and B. Deveaud-Plédran, Nat. Mater. **9**, 655 (2010).

[23] S. S. Gavrilov, N. A. Gippius, S. G. Tikhodeev, and V. D. Kulakovskii, JETP **110**, 825 (2010).

[24] Ö. Bozat, I. G. Savenko, and I. A. Shelykh, Phys. Rev. B **86**, 035413 (2012).

[25] S. S. Gavrilov, A. V. Sekretenko, S. I. Novikov, C. Schneider, S. Höfling, M. Kamp, A. Forchel, and V. D. Kulakovskii, Appl. Phys. Lett. **102**, 011104 (2013).

[26] S. S. Gavrilov, A. V. Sekretenko, N. A. Gippius, C. Schneider, S. Höfling, M. Kamp, A. Forchel, and V. D. Kulakovskii, Phys. Rev. B **87**, 201303 (2013).

[27] A. V. Sekretenko, S. S. Gavrilov, S. I. Novikov, V. D. Kulakovskii, S. Höfling, C. Schneider, M. Kamp, and A. Forchel, Phys. Rev. B **88**, 205302 (2013).

[28] S. S. Gavrilov, A. S. Brichkin, S. I. Novikov, S. Höfling, C. Schneider, M. Kamp, A. Forchel, and V. D. Kulakovskii, Phys. Rev. B **90**, 235309 (2014).

[29] T. Mori, Y. Yamayoshi, and H. Kawaguchi, Appl. Phys. Lett. **88**, 101102 (2006).

[30] K. Huybrechts, G. Morthier, and R. Baets, Opt. Exp. **16**, 11405 (2008).

[31] T. Elsass, K. Gauthron, G. Beaudoin, I. Sagnes, R. Kuszelewicz, and S. Barbay, Eur. Phys. J. D **59**, 91 (2010).

[32] D. Hayashi, H. Takahashi, T. Katayama, and H. Kawaguchi, J. Lightw. Technol. **32**, 2671 (2014).

[33] J. Zamora-Munt and C. Masoller, Opt. Exp. **18**, 16418 (2010).

[34] I. A. Shelykh, A. V. Kavokin, Y. G. Rubo, T. C. H. Liew, and G. Malpuech, Semicond. Sci. Technol. **25**, 013001 (2010).

[35] D. Ballarini, M. De Giorgi, E. Cancellieri, R. Houdré, E. Giacobino, R. Cingolani, A. Bramati, G. Gigli, and D. Sanvitto, Nat. Commun. **4**, 1778 (2013).

[36] R. Cerna, Y. Léger, T. K. Paraïso, M. Wouters, F. Morier-Genoud, M. T. Portella-Oberli, and B. Deveaud, Nat. Commun. **4**, 2008 (2013).

[37] W. L. Zhang, F. Wang, Y. J. Rao, R. Ma, and X. M. Wu, J. Lightw. Technol. **33**, 3933 (2015).

[38] S. S. Gavrilov and N. A. Gippius, Phys. Rev. B **86**, 085317 (2012).

[39] S. S. Gavrilov, A. A. Demenev, and V. D. Kulakovskii, JETP Lett. **100**, 817 (2015).

[40] T. C. H. Liew, A. V. Kavokin, and I. A. Shelykh, Phys. Rev. Lett. **101**, 016402 (2008).

[41] A. Amo, T. C. H. Liew, C. Adrados, R. Houdré, E. Giacobino, A. V. Kavokin, and A. Bramati, Nat. Photon. **4**, 361 (2010).

[42] C. Ciuti, P. Schwendimann, and A. Quattropani, Semicond. Sci. Technol. **18**, S279 (2003).

[43] S. S. Gavrilov, Phys. Rev. B **94**, 195310 (2016).

[44] S. S. Gavrilov, JETP Lett. **105**, 200 (2017).

[45] S. S. Gavrilov, Phys. Rev. Lett. **120**, 033901 (2018).

[46] L. A. Lugiato and R. Lefever, Phys. Rev. Lett. **58**, 2209 (1987).

[47] P. Parra-Rivas, E. Knobloch, D. Gomila, and L. Gelens, Phys. Rev. A **93**, 063839 (2016).

[48] M. A. Ferré, M. G. Clerc, S. Coulibally, R. G. Rojas, and M. Tlidi, Eur. Phys. J. D **71**, 172 (2017).

[49] M. G. Clerc, M. A. Ferré, S. Coulibaly, R. G. Rojas, and M. Tlidi, Opt. Lett. **42**, 2906 (2017).

[50] S. S. Gavrilov, Phys. Rev. B **90**, 205303 (2014).

[51] S. S. Gavrilov, A. S. Brichkin, Y. V. Grishina, C. Schneider, S. Höfling, and V. D. Kulakovskii, Phys. Rev. B **92**, 205312 (2015).